

DEVELOPMENT OF A MASS EVALUATION TOOL FOR CLASSICAL AND DISRUPTIVE AIRCRAFT STRUCTURES

Valentin PRIASSO¹, Antoine LANNOO¹

¹DMAS, ONERA, 59000, Lille, France

Abstract

This paper deals with a mass evaluation tool of an aircraft structure which uses semi-empirical and numerical models. It aims to be integrated into a Multidisciplinary Design Analysis and Optimization (MDAO) process for innovative aircraft. The optimization method is presented and some examples are detailed on both classical and disruptive aircraft structures.

Keywords: Structure, mass, optimization.

Nomenclature

BWB : Blended Wing Body FEA : Finite Element Analysis

MDAO: Multdisciplinary Design Analysis and Optimization

MLW: Maximum Landing Weight MTOW: Maximum Take-Off Weight

SBW: Strut-Braced Wing

TLAR: Top Level Aircraft Requirement

1. Introduction

1.1 Interest of mass prediction

Air traffic has been rising for many years. This growth is set to continue in the future, inevitably leading to an increase in aviation-related gas emissions. At the same time, the environmental stakes have never been higher, with numerous climate disturbances and natural disasters. It is therefore important to ensure that tomorrow's aircraft have the lowest possible impact on the environment. This involves innovations of various kinds, from materials (light composite), fuel (Sustainable Aircraft Fuels), improvement of the air traffic and new structures (Blended Wing Body (BWB)) to decrease the aircraft mass [1].

The optimization of an aeronautical structure, i.e. the minimization of its mass while ensuring that the aircraft can fulfil its intended functions without undergoing permanent strain or failure, involves many disciplines. During the aircraft development process, many disciplines are involved, such as propulsion, aerodynamics, structure and handling qualities. Each imposes design constraints on the overall geometry of the aircraft that must be respected by the others. To make the link between their results, MDAO process has been developed at ONERA – The French Aerospace Lab and in other laboratories [2-4]. It is composed of numerous disciplinary modules, integrating the strong disciplinary expertise of ONERA, in order to take into account the broadest possible criteria or parameters that could affect the aircraft design to obtain a feasible and realistic final solution. One of the inputs to this process is often the Maximum Take-Off Weight (MTOW), which influences all the discipline modules.

An accurate estimation of this mass is therefore necessary, as well as the inertia of the structure. Ideally, as all the parts of the aircraft have an influence on its performance, they all should be considered when calculating the mass. The model presented in this paper focuses on the wing as it is a major part of an aircraft and because other models and data already exist in the literature. We'll see in the last section that this method can be applied to the whole structure.

1.2 Aircraft wing mass evaluation methods

Many authors working on aircraft wing weight estimation methods have proposed classifications of these methods ([5-7]). Although these classifications are not identical, they are quite similar in that they often divide the methods into three categories according to their precision, complexity and time of use in the design process. As described in detail in ([8]), these categories are: empirical, analytical or based on Finite Element Analysis (FEA).

Empirical methods use data from existing aircraft structures. They relate the mass of the wing to its main properties, such as its surface area, wingspan and sweep angle. The accuracy of such a method is directly related to the quantity and quality of the available data, which can be found in some papers ([9]). It can be very effective for estimating the wing mass of a subsonic civil transport aircraft (with a standard Tube and Wing geometry) but will be of little use for designing an innovative structure (Blended Wing body (BWB)). Examples of empirical methods can be found in [10-12].

Analytical methods use the mechanics of materials to calculate the optimal shape/thickness of components required to ensure the structure's resistance to different stresses (e.g. bending and torsion). They use detailed wing geometry to achieve better results than empirical methods. However, the arrangement of internal components is not always considered, which can lead to inaccuracies in bending and torsion stiffness, and hence in stress calculations. Examples of analytical methods can be found in [13-15].

A finite element model of the complete structure provides a faithful representation of its behavior. This ensures accurate optimization of the wing components. Depending on the accuracy of the mesh (size, linear/non-linear), a compromise can be found between the accuracy of the result and the computational time. Some authors cleverly combine relatively coarse initial calculations (one-dimensional) to initiate optimization before performing a more precise analysis ([16]). However, these methods are often associated with the use of a finite element software, which could be a difficulty during the MDAO process (license availability). Examples of FEA methods applied to aircraft structure can be found in [16-18].

1.3 Our approach

The model, described in the next section, has been developed for integration into an MDAO process. In addition to providing a reliable result, it must be fast and not require the opening of external software. A full and detailed calculation of the structure using finite elements is therefore out of the question. Nevertheless, we will use the FEA with a relatively coarse 2D mesh coupled to material mechanics equations. Finally, in order not to be dependent on open source software, the FEA and the entire model were coded in Excel/VBA.

The Section 2 details the different steps of the model. The main assumptions made on both the geometry and the finite element model are explained. In the Section 3, the model is used to calculate the wing mass of different aircraft. We start with the study of existing aircraft with a classical tube and wing structure. To test the model on more complex geometries, the case of a Strut-Braced Wing (SBW) with a high aspect ratio is analyzed. ONERA has been working for around ten years on this kind of configuration, and is now evaluation its benefits for the future greener short-medium range aircraft in the frame of the Clean Aviation SMR ACAP project. Finally, disruptive BWB geometry analysis is also carried out. This will show the current limitations of the model and allow us to consider future improvements in the last section.

2. Description of our mass evaluation model

2.1 The different steps of the model

First, a brief overview of the method is given and illustrated in Figure 1. More details on each part of the method will be given in its own dedicated sub-section in this paper.

The first step in the model is to define the input data for the model. The user needs to specify the geometry of the wing (planform) as well as the Top-Level Aircraft Requirement (TLAR) of the aircraft (such as MTOW, load cases, Mach number).

As it is usually the case in the literature, the wing is divided into two distinct parts. One, called the primary structure, is analyzed using FEA. A mesh is generated and a loop is run between calculating the components stresses and optimizing their geometry. This optimization loop will end once an optimized mass has been reached. To determine the mass of the second part of the wing, called the secondary structure, semi-empirical formulae are used.

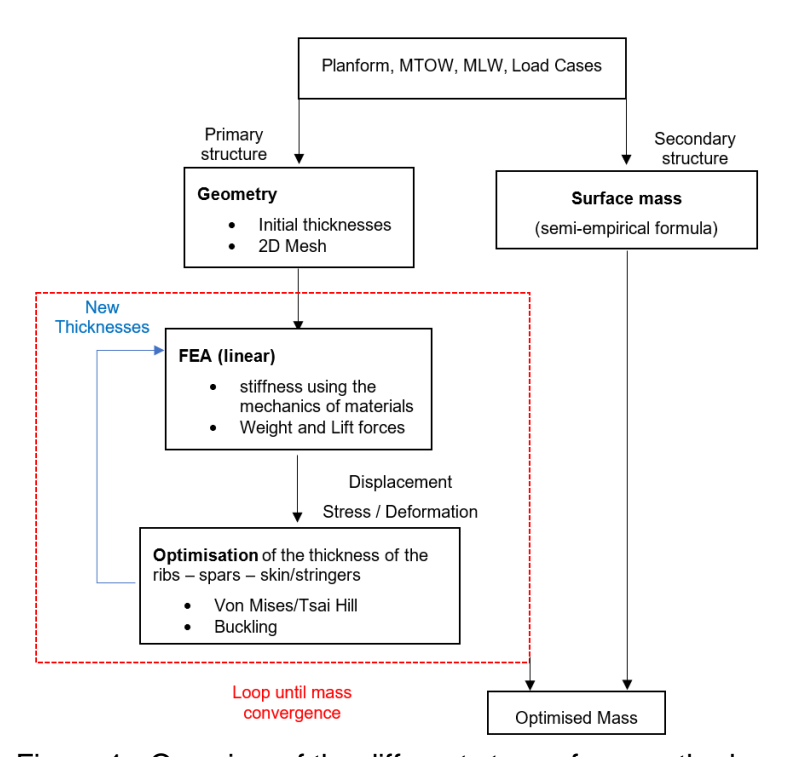


Figure 1 - Overview of the different steps of our method.

2.2 Description of the geometry

To calculate the mass balance of a wing, it is important to establish its geometry to represent the main components (left part of the Figure 2). Since the aircraft has an axis of symmetry, a single wing is dimensioned. First, the wing is divided into two parts: the primary structure and the secondary structure. The primary structure is the wingbox made up of ribs, front/rear spars and upper/lower skin-stringers. The secondary structure refers to the leading and trailing edges, with the various movable appendices such as ailerons, flaps and slats.

The planform of the wing is segmented into different sections. First, the root, where the fuselage merges with the wing. At the end of the wing is the tip, and between these two sections may be one or more kinks, which are points where the angle of the leading edge or trailing edge (or both) changes. For each of the sections, input data are used to model the wing such as the span. The airfoil is modelled using [19] and his chord and relative thickness. Between each section are established boxes, each with a twist angle and a dihedral as well as the sweep angle of the leading edge or the centering axis, depending on the project requirements. Finally, to establish the internal structure, the chordwise positions of the leading and trailing edges are requested.

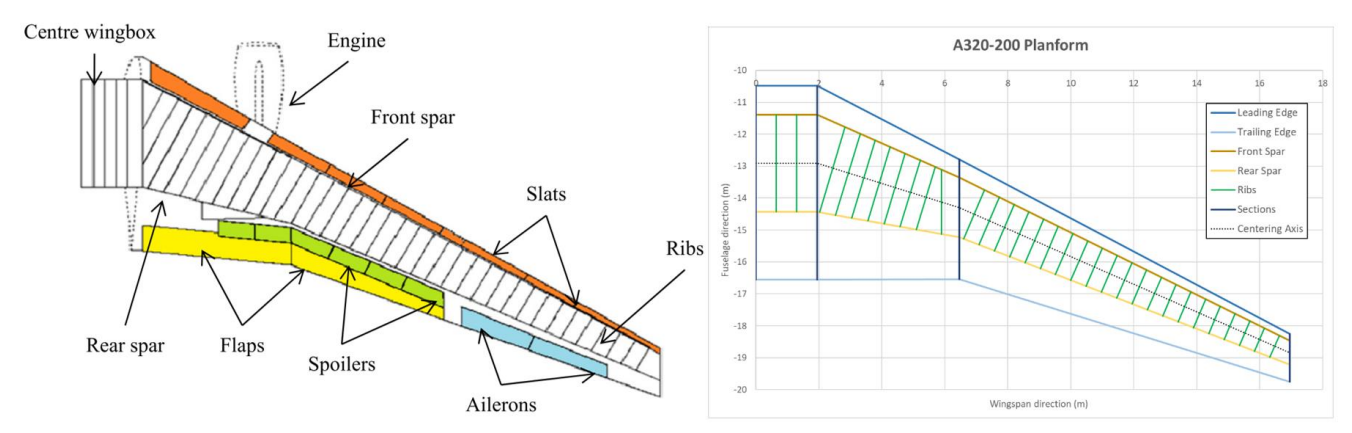


Figure 2 - Wing planform of a conventional transport aircraft. (Left: detail drawing [8], Right: model scheme).

From these data, the planform is drawn (right part of the Figure 2). Between two sections all the values vary linearly. As can be seen in Figure 2, the ribs are perpendicular to the central axis except at the section position and at the rib used to attach the engine which are parallel to the fuselage axis. The space between each rib is set at 50 centimeters, as is the space between the stringers (20 cm), which corresponds to conventional values [23]. The engine is not modeled, but it does contribute to the dimensioning of the wing as its mass is given as inputs and added as a punctual mass on the additional rib.

2.3 Finite elements analysis

Several methods can be used to calculate the stresses in the structure. Strength of materials equations provide a rapid but approximate analysis of the deformations undergone by the components. The use of the FEA provides more accurate results. Early versions of the code provided rapid simulation using beam elements. However, this one-dimensional modeling, while fast, could raise difficulties, particularly in terms of element torsion. For this reason, an enhancement has been made in the current model to enable using 2D shell elements.

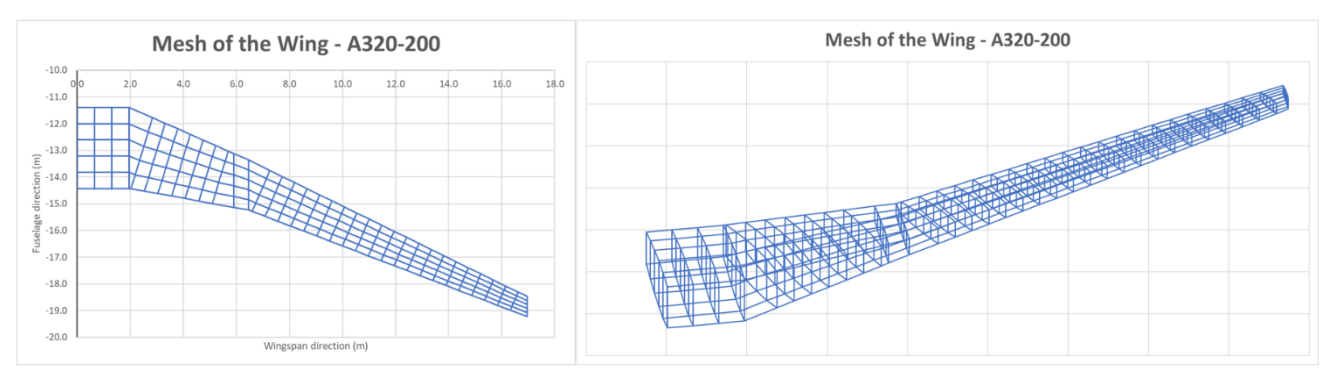


Figure 3 - Example of a mesh (Left: top view, Right: inclined view).

Each main component (skin, spar and rib) is modelled using shell elements. An example of a mesh is shown in the Figure 3. In the wingspan direction, there is at least one element between two successive ribs. In the chord direction, it is necessary to divide the segment into several elements to maintain a correct shape of the elements. A division of five elements along the entire wing, is chosen to correctly represent the skin surface without making the calculation too long. Finally, only one element is created in the thickness of the wing. The elements of the ribs and spars near to the root and the tip of the wing look a little slender. A better mesh would be to divide into two elements only near the root, but this solution has not yet been programmed. It should be noted that the stringers are not included in the mesh. Their properties such as bending stiffness are added directly to that of the skin elements via the stiffness matrix.

The 2D shell elements used are called Discrete Kirchhoff Triangle (DKT) or Discrete Kirchhoff Quadrilateral (DKQ). They are based on the Kirchhoff–Love theory of thin plates using the plane stress hypothesis [21,22].

The components can be made of isotropic material (aluminum alloy) or orthotropic (composite laminate) with elastic properties. In the case of laminates, the lay-up used respect the usual constraints imposed by the manufacturing and the experience (e.g. minimum proportion of 0° plies...) [23].

The linear FEA is perform from this mesh by adding a lift force distributed elliptically along the span of the wing. In the current model, only symmetric load cases are considered with load factors of +3.75 and -1 and a safety factor of 1.5.

2.4 Optimization

A first FEA is performed with initial thickness of components of 5 mm. The stresses are then computed. As the FEA is linear, the integrity of the structure is controlled after the simulation. So the next step is to determine if there is a break (in the case of composite material), plasticity (in the case of aluminum for example) or buckling of the main components of the wing. These criteria will be checked on each component and its thickness will be optimized to guaranty the integrity of the structure. The thickness can change from one spar/rib/skin to the other so that every wingbox has its own optimized geometry.

For every element using isotropic material, the Von Mises yield criterion is computed ([24]). In the case of laminates, the Tsai-Hill failure criterion is used for each ply ([25]). In case of a failure, the thickness of all the plies is slightly increased.

To verify that no local buckling occurs on the components, mechanics of materials equations are used. The skins, spars and ribs are modelled as plates undergoing membrane stresses (longitudinal, transverse and shear). We then use equations from the literature to determine the critical load of this thin plate under combined loading ([26,27]). Finally, for the buckling of the beam, the critical loads are well-known in the literature. Depending on the beam radius of gyration, length and boundary conditions, the global buckling or local one (called crippling) can be predicted. The equations can be found in [28].

2.5 Secondary structure

As previously mentioned, the secondary structure represents the various leading and trailing edge components. No finite element calculations are performed directly on these edges, but their masses are calculated using semi-empirical formulae based on civil transport tube and wing aircraft from the literature [12]. So, for each box, the type of edge element involved (slat, aileron, etc.) change its surface mass. This mass depends on the following parameters of the aircraft:

Leading and trailing edge boxes: function of the MTOW

Slats: function of the wing loading

Ailerons: function of the diving speed

Spoilers: constant valueFlaps: function of the MLW

3. Application of the model

3.1 Classical geometry of Tube-and-Wing

In order to verify the quality and consistency of our model, it is used to calculate the wing mass of aircraft known from the literature. Based on the geometries detailed in [8], we chose four of the aircraft shown in the Table 1. This list includes three medium range aircraft (MTOW < 100 tons) with a wingspan of around 35 meters, and one long range with a MTOW around 140 tons and a wingspan of 43.9 meters. The three Airbus aircraft have wing-mounted engines but the engines of the B727-200 are located at the rear of the fuselage.

Name	MTOW (tons)	WingSpan (m)	Aspect Ratio
A320-200	73.5	33.9	9.38
B727-200	78.019	32.9	6.65
A321-200	83	34.9	9.96
A310-200	138.6	43.9	8.8

Table 1: Main properties of the studied aircrafts.

The material used in the model is an Al-Li Alloy 2099-T83 with the following properties: Young modulus (78 GPa), yield strength (590 MPa) and density (2 630 kg/m³). This material is representative of the one used in the four aircraft presented. These aircraft are made up of very few composite materials (less than 10% for the Airbus A310 and A320) and are mainly distributed over the secondary wing structure.

As the internal structure of the wings was not specified, the same spacing between ribs and stringers was used (50 and 20 cm respectively). The same for the front spar (15% of the chord length from the leading edge) and the rear spar (65%). The airfoils used are NACA 2301 for the Airbus, and BAC XXX for the Boeing aircraft (http://airfoiltools.com/).

With regard to the secondary structure, since it is difficult to find the exact position of the high-lift devices, only the primary structure has been modelled. The mass of the structure thus obtained should be less than the theoretical value for the same proportion between configurations. To estimate the total mass of the wing, we make the hypothesis that the secondary structure has a mass representing about 25% of the total mass, which is an estimation found in the literature ([8,12]).

Name	Real mass of	Computed mass of	Computed mass	Relative Difference
	the wing ([9])	the primary	of the wing	Model - Real
	(tons)	structure (tons)	(tons)	(%)
A320-200	8 766	5 851	7 802	-12
B727-200	8 956	9 893	13 190	+47
A321-200	10 026	6 794	9 059	-10
A310-200	18 496	15 457	20 608	+11

Table 2: Computed wing mass.

The results are presented in the Table 2. The real mass of the wing is from the literature [9]. It appears that, in three cases out of four, the model manages to predict quite well the wing mass (less than 12% of relative difference). The case of the B727-200 stands out, however, having been overestimated by almost 50%. One explanation could be the low aspect ratio of the wing. It could make the hypothesis of an elliptical distribution of lift less accurate than in the other three cases. Another explanation could be a difference of the internal structure of the wing between an Airbus aircraft and one of Boeing. Further computation of the wing mass of other Boeing aircraft are currently performed to verify this.

3.2 Strut-Braced Wing (SBW)

Having compared our model with existing models to assess its relevance, it is now possible to carry out trend studies on innovative models. One of the layouts tested with the code is the strut-braced wing. The SBW's main advantage lies in its strut, which supports part of the stresses applied to the wing, thus reducing strain. This enables the wing's aspect ratio, for example, to be increased while reducing the mass of its structure, thus reducing the aircraft's fuel consumption. Another advantage of this configuration is that it's close to the classical Tube-and-Wing, making it a good entry point into innovative design geometries for our tool.

The first test carried out on the SBW is the study of the spanwise position of the link between the strut and the wing. Obviously, the further away the connector is from the fuselage, the longer and heavier the strut will be. However, this will have an impact on the wing's strength, and therefore on its weight. This is why the total mass (wing plus strut) is analyzed. Wing-tip deformation is also studied. As the study focuses exclusively on the position of the strut link, the external geometry of the main wing remains unchanged, and only its internal structure is optimized. The code enables the user to choose between a fixed and a pivoting connection. For this study, the choice has been made to fix the strut at both ends.

According to the work carried out for the U-HARWARD Project [29], it would seem that the optimum position for reducing total wing mass is at 2/3 of its span. We therefore took this value as a reference and varied the studied spans around it. The values obtained are plotted in Figure 4. For each of the span values used, the sum of the lift forces acting on the surface between the wing root and the strut attachment has been calculated. The liftwise position is therefore the ratio of this force to the total lift force acting on the wing.

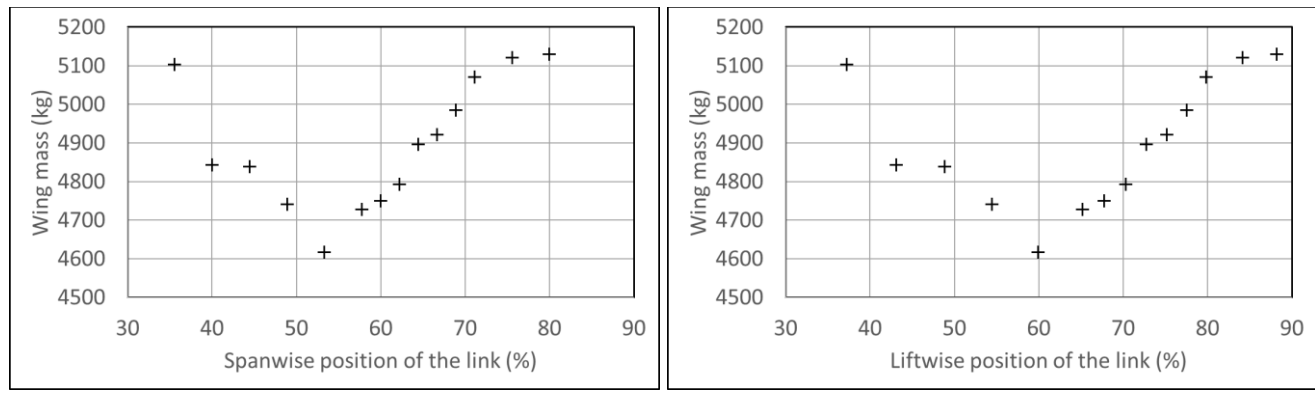
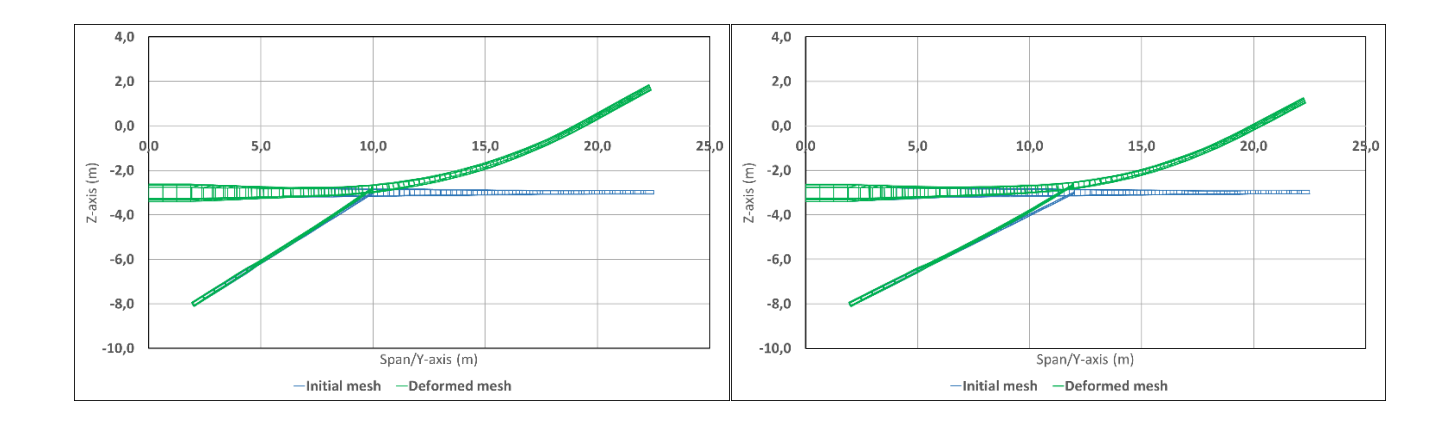


Figure 4 - Wing mass for different spanwise and liftwise positions.

The deformation of the wing (which measures 22.5m) and the strut has been plotted in Figure 5 for different span values (10, 12, 14 and 16m) to visualize the behavior.



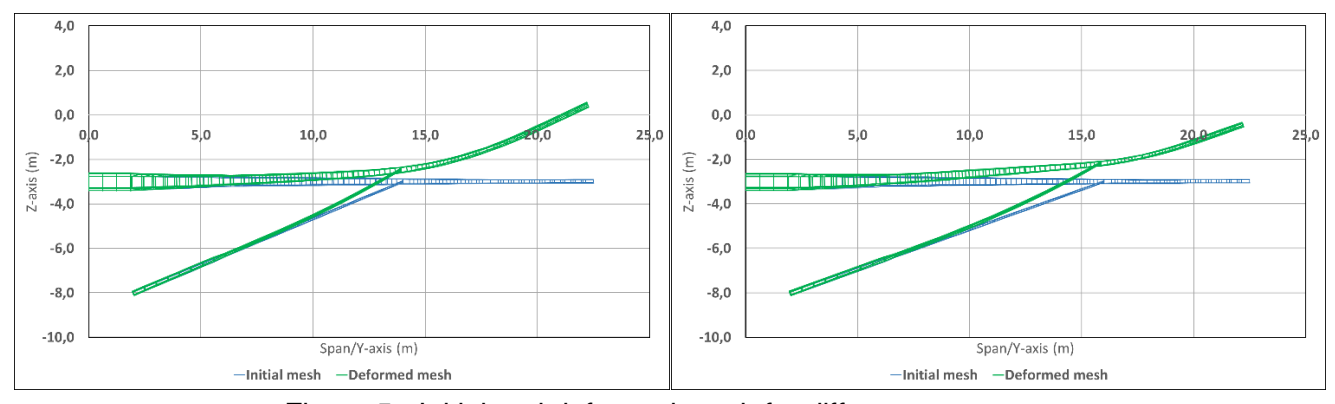


Figure 5 - Initial and deformed mesh for different strut cases.

Two conclusions can be reached from these figures and results. The first is that the further the link between the wing and the strut is located spanwise, the smaller the wing's deformation will be. The second is that there is an optimum distance for which the total mass of the wing is the lowest. In the example, this distance is between 50 and 55% spanwise and around 60% liftwise, which is a bit different than the 2/3 value found in the literature. It may be interesting to see whether these values remain the same for different wing and strut configurations and, if not, what links exist between this position and the different geometries.

This comparison with existing literature allows us to define the limits and possible improvements for our study, but also for our code. One of the limits of this study is that it has only been carried out for a strut in tension (for a load factor of 3.75). In certain load cases, the strut may end up in compression, and this will have an impact on its design and optimization as the global buckling of the strut can occur.

3.3 Disruptive structures BWB

Our model has also been tested on innovative BWB structures. This geometry has been widely studied over the last decades as it offers a promising aircraft with low fuel consumption [30-33]. Such a structure is classically divided into three zones: the central body, the transition zone and the wing (Figure 6). The central body is the main part of the aircraft and contains the passenger cabin and the cargo hold. It is the pressurized part of the BWB. The transition zone is the link between the central body and the wing. Finally, the wing is very similar to that of Tube-And-Wing, with an internal structure made up of ribs, spars, skin and stringers.

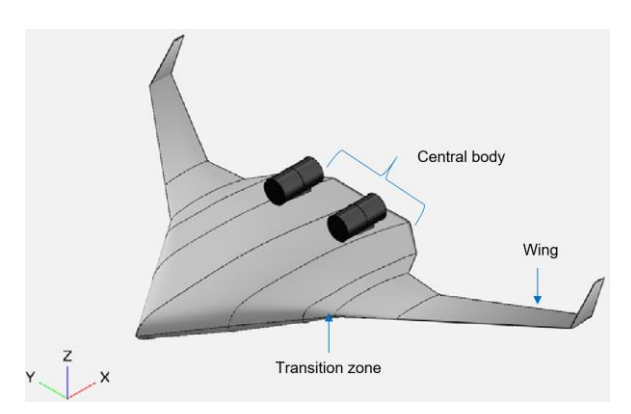


Figure 6 - Example of a BWB configuration.

Computing the mass of such an aircraft is challenging as there is no comparison data from a real structure. In this section we will compare our model, adapted to the specificities of the flying wing, to the results from the paper [34]. The test configuration used is the Boeing BWB-450-1L, with a seating capacity of 450 passengers. Thanks to a detailed FEA, the authors computed the mass of the primary structure using the Nastran SOL 200 optimizer. The dimensions of the aircraft and the structural layout used in [34] are presented in the Figure 7.

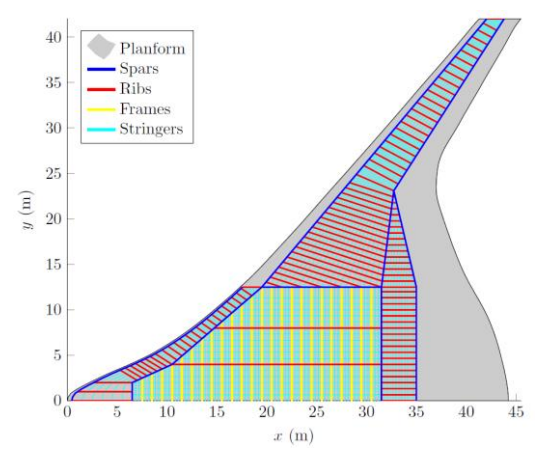


Figure 7 - Boeing BWB-450-1L structural layout (from [33]).

The pressurized part of the BWB is delimited by upper and lower skins which are quite flat. Unlike the circular fuselage of a tube-and-wing, the pressure forces will add bending moment to the skin in addition to the membrane forces. A stress gradient will therefore be present in its thickness, as well as compression forces. It is therefore necessary to use frames in the X and Y directions (I cross section beam) to reinforce the skin. Finally, stringers are added to the skin to prevent excessive local deformation of the panel located between two frames. The stringers height is less than the one of the frames to save mass while still adding bending stiffness.

In addition to this pressure, the central body also transmits bending forces between the two wings. These forces will be neglected and the sizing of the central body is done using only a differential pressure of 63 kPa.

The optimization of the skin and the frames is done to prevent a large deflection of the components (less than 10% of vertical displacement compared to the length) and to prevent the failure. The parameters used to minimize the mass while ensuring these conditions are the spacing between the frames, between the stringers and their height. The thickness of the skin is set to 4 cm.

To compute the deformation of the components, equations from the mechanics of material are used. The frames are considered as beams simply supported under an uniform pressure load. The reinforced skin is modelled as a flat plate which size correspond to the spacing of the X and Y frames. A loop on each of the five parameters is done to get the geometry with the lowest surface mass.

To compute the mass of the transition part, the same properties of the optimized central body are used. This hypothesis will probably over-estimate its mass as this section is not pressurized and undergoes only bending moment from the wing. A more detailed analysis is being developed in the futur model. Finally, the mass of the wing can be computed using the same model as the one presented in the Section 2 of this paper.

In the Table 3 are presented the results. The comparison with [34] is quite satisfactory as the central body and transition mass is over-estimated by our model by 15% and the wing mass under-estimated by 4%.

Table 3 - Comparison of the mass (kg) of the primary structure of the BWB-450-1L between the results from [5] and our model.

Masse of the aircraft parts (kg)	Paper [34]	Our model	Relative difference (%)
Centrale body and transition zone	48 472	55 631	+ 15
Wings	17 684	17 030	- 4

The mass breakdown of both parts is also detailed in the [34]. For the central part, it is difficult to compare to our result as the authors didn't make the distinction between central body and the transition zone. We can however do the comparison for the wing in Figure 8. It can be seen that even if the global mass of the primary structure of the wing is similar, the repartition is quite different.

First, the mass of the ribs is about 20% higher in our model. It can be explained by the spacing between two consecutive ribs that is different. In our model a constant space of 60 cm is used, but in the paper this space value increases from the root up to 90 cm at the tip. The number of ribs is therefore more important in our model. It might explain the difference but we should keep in mind that even if there are more ribs, if their thicknesses is less important the global mass could be the same. A more detailed comparison of the evolution of the thickness of the ribs would be necessary to explain the difference. The other components of the wing, skin/stringers and spars, contribute to the bending stiffness. In our model, the spars only represent 6% of these components while in the paper the proportion is around 22%. The number of stringers used could be an explanation. It is not specified in the paper but in our model a space of 20 cm is set. If this space is lower than in the paper, the stringers in our model will be more efficient to resist the bending so the spars will need a lower thickness.

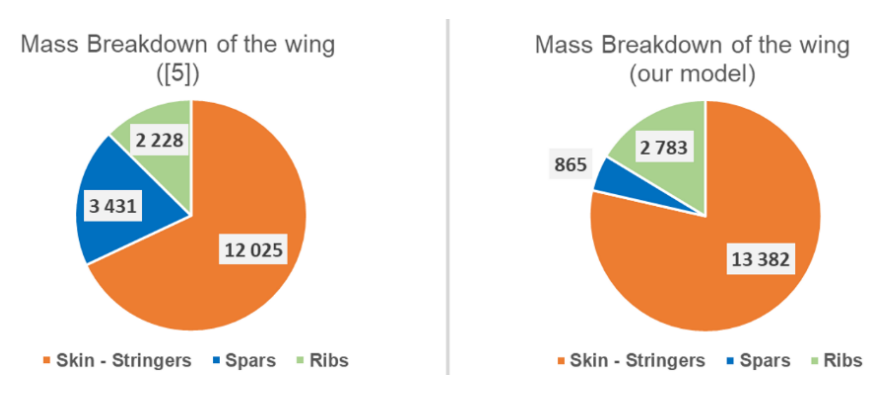


Figure 8 - Comparison of the mass breakdown of the wing.

This comparison of our model result with a high-fidelity model from the literature is encouraging. The mass of the wings is similar, even though the internal structure may be different, and the global mass of the primary structure is comparable. Many improvements can be made on the model. The first will be to create a finite element analysis of the central body to get the stresses on the components more accurately. The transition zone needs also to be more detailed with the specific optimization of its components to resist the bending forces. Finally, the secondary part represents a significant proportion of the global mass of the BWB. As there is not a lot of empirical data on these parts, a careful model of it needs to be created.

4. Conclusion and perspectives

4.1 Conclusion

Tools have been developed within ONERA to support MDAO projects. One of these tools provides mass balance and optimization of Tube-and-Wing structures, as well as innovative structures. It is based both on material mechanics calculations and on a finite element model for the primary structure and on statistical formulae for the secondary one. The combination of these different aspects enables rapid assessment and optimization, which can be integrated into MDAO loops.

To ensure the relevance of the model, comparisons were made with existing aircraft data. The results are quite encouraging (about 10% difference with the real mass of three aircraft) although one configuration tested requires further investigation.

Once the code had been compared and improved, it was possible to study innovative structures such as the Strut-Braced Wing with a high aspect ratio or the Blended Wing Body. For the SBW, the study of the spanwise position of the connection between the strut and the wing shows an optimum position around 55-60% of the spanwise. This interesting result can help to better select the positioning range of the strut during the MDAO process. Finally, the model was used to compute the mass of the Boeing BWB-450-1L, a BWB configuration studied with a high-fidelity model in [33]. A comparison of our results with those of that paper shows a difference of -4% for the wing mass and an overestimation of +15% for the mass of the central body and the transition zone. For this last part, although the use of equations from the mechanics of material gives a fairly accurate estimate, the complexity of the structure requires a more detailed model. The use of a simple FEA on this part is therefore being considered to improve our model.

4.2 Limit and perspectives of the model

Initial use of the model presented in this paper has shown satisfactory results. However, many assumptions have been made that can be improved. The two most important ones are being changed in the future model.

The first concerns the distribution of the lift forces. The elliptical distribution used so far does not allow us to represent the variation of aerodynamic forces along the chord of the wing. This approximation may have its limitations for wings with large chords or when maneuvering with deflected ailerons. The use of the vortex lattice method would improve the representation of the aerodynamic loads and therefore the accuracy of the results.

The second simplification concerns the material. The model can currently optimize the thickness of isotropic materials. For a composite material, we can simulate a laminate but not optimized it. Even if we limit ourselves to four ply directions (0, 90 and +-45), finding the optimum stack requires advanced methods. In a future improvement of our model, we will restrict ourselves to predefined stacking sequences in order to limit the number of possibilities.

5. Contact Author Email Address

valentin.priasso@onera.fr antoine.lannoo@onera.fr

This work is co-funded by the European Union under Grant Agreement number 101101955. Views and opinions expressed are however those of the author(s) only and do not necessarily reflect those of the European Union or Clean Aviation Joint Undertaking. Neither the European Union nor the granting authority can be held responsible for them.





6. Copyright Statement

The authors confirm that they, and/or their company or organization, hold copyright on all of the original material included in this paper. The authors also confirm that they have obtained permission, from the copyright holder of any third party material included in this paper, to publish it as part of their paper. The authors confirm that they give permission, or have obtained permission from the copyright holder of this paper, for the publication and distribution of this paper as part of the ICAS proceedings or as individual off-prints from the proceedings.

References

- [1] Bergero C, Gosnell G, Gielen D, Kang S, Bazilian M and Davis S.J. (2023). Pathways to net-zero emissions from aviation. *Nature Sustainability*, 6(4), 404-414.
- [2] Gauvrit-Ledogar J, Tremolet A, Moens F, Meheut M, Defoort S, Liaboeuf R, Morel F and Paluch B. Multidisciplinary Design Analysis and Optimization Process dedicated to Blended Wing Body Configurations. In Proceedings of the *33rd Congress of ICAS*, Stockholm, Sweden, 4–9 September 2022
- [3] Gray JS, Hwang J.T, Martins J.R, Moore K.T and Naylor B.A (2019). OpenMDAO: An open-source framework for multidisciplinary design, analysis, and optimization. *Structural and Multidisciplinary Optimization*, *59*, 1075-1104.
- [4] Dababneh O. (2016). Multidisciplinary design optimisation for aircraft wing mass estimation.
- [5] Murphy N.A.D. (1987). Analytical wing weight prediction/estimation using computer based design techniques.
- [6] Chambers M.C, Ardema M.D, Patron A.P, Hahn A.S, Miura H and Moore M.D. (1996). *Analytical fuselage and wing weight estimation of transport aircraft* (No. NASA-TM-110392).
- [7] Elham A. (2013). Weight indexing for multidisciplinary design optimization of lifting surfaces.
- [8] Dababneh O and Kipouros T. (2018). A review of aircraft wing mass estimation methods. *Aerospace Science and Technology*, 72, 256-266.
- [9] Roux É. (2005). Pour une approche analytique de la dynamique du vol. *These*, *SUPAERO-ONERA*.
- [10] Raymer D. (2012). Aircraft design: a conceptual approach. American Institute of Aeronautics and Astronautics, Inc..
- [11] Roskam J. (1989). Airplane Design: Part II. Preliminary Configuration Design and Integration of the Propulsion System.
- [12] Torenbeek E. (1982). Synthesis of Subsonic Airplane Design. Delft, Netherlands.
- [13] Torenbeek E. (1992). Development and application of a comprehensive, design-sensitive weight prediction method for wing structures of transport category aircraft. *Delft University of Technology, Faculty of Aerospace Engineering, Report LR-693*.
- [14] Howe D. (1996). The prediction of aircraft wing mass. *Proceedings of the Institution of Mechanical Engineers, Part G: Journal of Aerospace Engineering*, 210(2), 135-145.
- [15] Ajaj R.M, Friswell M.I, Smith D and Isikveren A.T. (2013). A conceptual wing-box weight estimation model for transport aircraft. *The Aeronautical Journal*, *117*(1191), 533-551.
- [16] Bindolino G, Ghiringhelli G, Ricci S and Terraneo M. (2010). Multilevel structural optimization for preliminary wing-box weight estimation. *Journal of Aircraft*, *47*(2), 475-489.
- [17] Hürlimann F, Kelm R, Dugas M, Oltmann K and Kress G. (2011). Mass estimation of transport aircraft wingbox structures with a CAD/CAE-based multidisciplinary process. *Aerospace Science and Technology*, *15*(4), 323-333.
- [18] Mitchell P.M. (1993). Advanced finite element weight estimation process on the high speed civil transport. *SAWE Paper*, 2169.
- [19] Sobieczky H. (1999). Parametric airfoils and wings. In *Recent development of aerodynamic design methodologies: inverse design and optimization* (pp. 71-87). Wiesbaden: Vieweg+ Teubner Verlag.
- [20] Sensmeier M and Samareh J. (2004, April). A study of vehicle structural layouts in post-WWII aircraft. In 45th AIAA/ASME/ASCE/AHS/ASC Structures, Structural Dynamics & Materials Conference (p. 1624).
- [21] Batoz J.L and Dhatt G. (1990). Modélisation des structures par éléments finis. Presses Université Laval.
- [22] Batoz J.L, Bathe K.J and Ho L.W. (1980). A study of three-node triangular plate bending elements. *International journal for numerical methods in engineering*, 15(12), 1771-1812.
- [23] Carpentier A. (2008). Optimisation multi-niveaux de panneaux composites (Doctoral dissertation, Toulouse 3).
- [24] Mises R.V. (1913). Mechanik der festen Körper im plastisch-deformablen Zustand. *Nachrichten von der Gesellschaft der Wissenschaften zu Göttingen, Mathematisch-Physikalische Klasse*, 1913, 582-592.
- [25] Azzi V.D and Tsai S.W. (1965). Anisotropic strength of composites: Investigation aimed at developing a theory applicable to laminated as well as unidirectional composites, employing simple material properties derived from unidirectional specimens alone. *Experimental mechanics*, *5*, 283-288.
- [26] Dima I. (2015). Buckling of flat thin plates under combined loading. *Incas Bulletin*, 7(1), 83.
- [27] Dubbel H. (2013). Dubbel-Handbook of mechanical engineering. Springer Science & Business Media.
- [28] Maddux G.E, Vorst L.A, Giessler F.J and Moritz T. (1969). Stress analysis manual. *Dayton: Technology Incorporated*.
- [29] Cooper J.E, Gu H, Ricci S, Toffol F, Adden S, Meheut M., ... and Barabinot, P. (2024). CS2-THT U-HARWARD Project: Final Assessment and Project Outcomes Evaluation. In *AIAA Scitech 2024 Forum* (p. 2111).
- [30] Liebeck R.H. (2004). Design of the blended wing body subsonic transport. *Journal of aircraft*, 41(1), 10-25.
- [31] Kimmel W.M and Bradley K.R. (2004). A Sizing Methodology for the Conceptual Design of Blended-Wing-Body Transports (No. NASA/CR-2004-213016).

- [32] Gauvrit-Ledogar J, Tremolet A, Defoort S, Morel F, Liaboeuf R and Méheut M. (2022, June). Multidisciplinary Design and Optimization of the Blended Wing Body Configuration SMILE. In 9TH EUROPEAN CONFERENCE FOR AERONAUTICS AND SPACE SCIENCES (EUCASS 2022).
- [33] Gauvrit-Ledogar J, Tremolet A and Brevault L. (2020). Blended wing body design. *Springer Optimization and Its Applications*, 385-419.
- [34] Qian J and Alonso J.J. (2018). High-fidelity structural design and optimization of blended-wing-body transports. In 2018 Multidisciplinary Analysis and Optimization Conference (p. 3739).